Original Paper

A Method for Generating Random Vibration Considering Kurtosis Response Spectrum

Daichi NAKAI[*, **] and Katsuhiko SAITO[*]

A random vibration test is important for confirming the safety of packaging when transporting goods on a truck bed. There are differences between the traditional random vibration method and real vibration measured on the truck bed. These differences may result in overpackaging or underpackaging. Therefore, improving the input vibration during vibration testing is an important theme. In this study, we focused on the kurtosis response spectrum. A previous study showed that the response kurtosis under the real vibration varies depending on the natural frequency. Therefore, it is assumed that a random vibration with the same kurtosis response spectrum as the real vibration is similar to the real vibration. We propose a new method for generating random vibration considering the kurtosis response spectrum. Vibrations with the same power spectral density, root mean square of acceleration, acceleration kurtosis, and velocity kurtosis (but different kurtosis response spectra) were generated by the proposed method and the previous study method. Comparing the kurtosis response spectra between the real and generated vibrations, the proposed method showed a particular improvement in the input vibration, especially when the damping factor was small.
Keywords: Transportation, Vibration test, Response Spectrum, Kurtosis

1. Introduction

A random vibration test is important for confirming the safety of packaging when transporting goods on a truck bed or railway car. In the traditional vibration method, the power spectral density (PSD) of the acceleration is only considered as a test condition. However, it has been pointed out that there are differences between real vibration on the truck bed and random vibration generated by the traditional method. Real vibrations on a truck bed are non-stationary because there are fluctuations in the truck driving speed and road roughness [1]. The traditional vibration method cannot reproduce this non-stationary condition. These differences may result in overpackaging or underpackaging because of inappropriate evaluation of antivibration requirements. Therefore, it is important to improve the random vibration during vibration testing.

Many studies have focused on the acceleration kurtosis (K_a) and the probability density of acceleration. The K_a value of a random vibration generated by the traditional method is 3, and the probability density of acceleration is the Gaussian distribution. On the other hand, the K_a values of real vibrations are usually leptokurtic (i.e., greater than 3) [2, 3]. Therefore, it is assumed that a random vibration with the same K_a as the real vibration is more similar to the real vibration than the one generated by the traditional method.

Rouillard proposed a method for generating random vibration with a non-Gaussian probability density distribution by combining Gaussian oscillations with different intensities [4]. Furthermore, Rouillard et al. proposed a method that considered the moving RMS of acceleration [5]. Winterstein proposed a method to transform a Gaussian vibration into non-Gaussian vibration using a Hermite polynomial [6]. Hosoyama et al. proposed a method for generating leptokurtic random vibration based on the phase differential [7]. Our previous study proposed a method for controlling not only K_a but also the velocity kurtosis K_v. It shows the effect of K_v on packaging damage using a single degree of freedom (SDOF) model [8].

* Transport Packaging Laboratory, Kobe University, 5-1-1, Fukaeminami, Higashinada, Kobe 658-0022, Japan
** Sankyu Inc. 16-1 Tsukiji, Yahatanishi, Kitakyushu, 806-0001, Japan
Corresponding author: Daichi Nakai. Tel: 093-645-7262 E-mail: d.nakai@sankyu.co.jp

As mentioned above, the proposed methods for improving random vibration mainly considered K_a, K_v, the probability density of the acceleration, the probability density of the velocity, and the moving RMS.

Hosoyama et al. proposed the kurtosis response spectrum as a characteristic of vibration for packaging [9]. Fig. 1 shows the schematic diagram of the response spectrum. The response spectrum assumes the SDOF model and is used to investigate the effects of vibrations at various natural frequencies. To obtain the response spectrum, the SDOF model response and its summary statistics (e.g., maximum, standard deviation, and kurtosis) are calculated many times with varying natural frequencies and damping factors under the random vibration or the real vibration measured on the truck bed. It is also shown that the kurtosis response spectrum varies with the natural frequency f_n of the SDOF model when the input vibration is the real vibration measured on the truck bed.

It is assumed that a random vibration with a kurtosis response spectrum that is the same as that of the real vibration is similar to the real vibration. In this study, we propose a method for generating the random vibration considering the kurtosis response spectrum. The relative displacement was used as the response of the SDOF system because it is proportional to the strain of the product. Then, the generated vibrations were compared with the real vibrations and the proposed method was much similar to the real vibrations than those in the previous study method, especially in the case of a small damping factor.

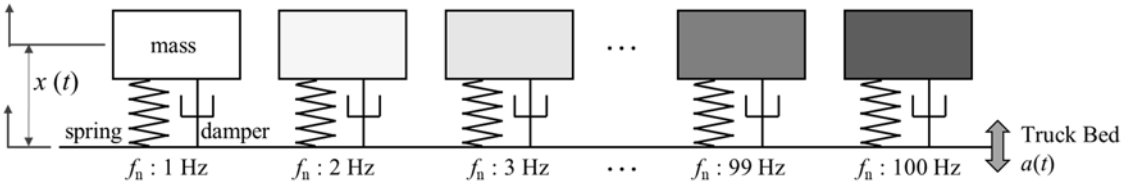

Fig. 1 Schematic diagram of response spectrum.

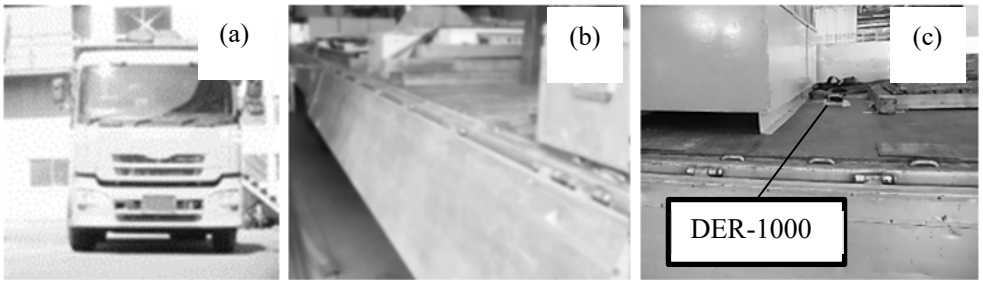

Fig. 2 Photos during the truck shipping experiment, (a) the truck taken from the front, (b) truck bed, (c) accelerometer.

2. Experiment

The vertical vibration data for the truck bed were used as a target. Fig. 2(a) and (b) shows the truck used for testing and truck bed, respectively. An accelerometer (DER-1000, Shinyei Technology Co., Ltd.) was fixed to the truck bed (Fig. 2(c)). We ran the truck on the highway for 1,200 s (low-pass filter, 100 Hz).

3. Calculation

3. 1 Method for calculating response spectrum

The acceleration applied inside the SDOF structure $a_i(t)$ are calculated using the same method as our previous study [8]. A SDOF system like that in Fig. 1 is expressed by equation (1):

$$m\left(\frac{d^2x(t)}{dt^2}+a(t)\right)+c\frac{dx(t)}{dt}+kx(t)=0, \quad (1)$$

where t, m, c, k, and $x(t)$ are, respectively, time, the mass, viscosity coefficient, spring constant, and the relative displacement between the mass and the truck bed. An impulse response function of the relative displacement $h(t)$ is expressed by equation (2):

$$h(t)=\frac{1}{\omega_{\mathrm{d}}}e^{-\zeta\omega_{\mathrm{n}}t}sin\omega_{\mathrm{d}}t, \quad (2)$$

where ω_{n}, ω_{d}, and ζ are, respectively, undamped natural angular frequency, and damped natural angular frequency of the response and the damping factor [10]. Meanwhile, ω_{n} is expressed by equation (3):

$$\omega_{\mathrm{n}}=2\pi f_{\mathrm{n}}=\sqrt{\frac{k}{m}} \quad (3)$$

The damping factor, ζ is expressed by equation (4):

$$\zeta=\frac{c}{2m\omega_{\mathrm{n}}} \quad (4)$$

The damped natural angular frequency, ω_{d} is expressed by equation (5):

$$\omega_{\mathrm{d}}=\omega_{\mathrm{n}}\sqrt{1-\zeta^2} \quad (5)$$

$x(t)$ is expressed by the equation (6):

$$x(t)=\int_o^t a(\tau)h(t-\tau)d\tau, \quad (6)$$

where τ is a parameter. Equation (6) is a convolution integral; therefore, $x(t)$ can be calculated by equation (7):

$$x(t)=\frac{1}{2\pi}\int_{-\infty}^{\infty}A(f)H(f)e^{2i\pi ft}\,df, \quad (7)$$

where $A(f)$ and $H(f)$ are the Fourier transform of $a(t)$ and $h(t)$, respectively. $a_{\mathrm{i}}(t)$ is proportional to the relative displacement $x(t)$:

$$a_{\mathrm{i}}(t)=\frac{k}{m}x(t)=4\pi^2f_{\mathrm{n}}^2x(t) \quad (8)$$

Here, f_{n} is from 1 to 100 Hz at intervals of 1 Hz. The RMS and kurtosis of $a_{\mathrm{i}}(t)$ calculated for each natural frequency f_{n} by fixing the damping factor with ζ, are the RMS response spectra $R_\zeta(f)$ and the kurtosis response spectra $K_\zeta(f)$.

3. 2 Methods for generating random vibration

3. 2. 1 Previous method

The traditional method for generating random vibration is expressed by equation (9):

$$a(t) = \sum_{k=1}^{L} A_{\mathrm{k}} \cos(2\pi \Delta f t + \phi_{\mathrm{k}}) \qquad (9)$$

where L, A_{k}, Δf, and ϕ_{k} are, respectively, the number of frequency components, amplitude, frequency resolution, and the k_{th} phase angle. A_{k} is expressed by equation (10):

$$A_{\mathrm{k}} = \sqrt{2\pi \Delta f P(k\Delta f)}\,, \quad (10)$$

where $P(k\Delta f)$ is the PSD. In traditional random vibration tests, ϕ_{k} denotes random numbers ranging from 0 to 2π.

When the random vibration was generated by the traditional method, ϕ_{k} and $\phi_{\mathrm{k-1}}$ were independent from each other. The method for generating a random vibration with arbitrary K_{a} by controlling the phase differences between ϕ_{k} and $\phi_{\mathrm{k-1}}$ is proposed [7]. The relationship between ϕ_k and ϕ_{k-1} is expressed by equation (11):

$$\phi_{\mathrm{k}} - \phi_{\mathrm{k-1}} = 2\pi \Delta f t_{\mathrm{gr}}(k\Delta f), \quad (11)$$

where $t_{\mathrm{gr}}(k\Delta f)$ is a group-delay time. $t_{\mathrm{gr}}(k\Delta f)$ is taken as a random number with an average value m and a standard deviation σ, and σ is related to the sharpness of the envelope curve. As σ decreases, the envelop curve becomes sharper and K_{a} increases. As σ increases, K_{a} converges to 3 (Gaussian). Our previous study showed that Δf also had an effect on the envelope curve and was related to the period T_{d} during which the maximum acceleration occurred [8]. The relationship between Δf and T_{d} is expressed by equation (12):

$$T_{\mathrm{d}} = \frac{1}{\Delta f} \quad (12)$$

When T_{d} is small, the ratio $K_{\mathrm{v}}/K_{\mathrm{a}}$ is less than 1. With increasing T_{d}, the ratio $K_{\mathrm{v}}/K_{\mathrm{a}}$ converges to one. In this study, T_{d} was set to 16 s in the case of the proposed method and 2 or16 s in the case of the previous method.

3. 2. 2 Proposed method

In the previous method, the standard deviation σ was a constant value, regardless of the frequency. In this study, the standard deviation of $t_{\mathrm{gr}}(k\Delta f)$ is not a constant value σ but a variable $\sigma_\zeta(f)$ that changes with frequency. In order to set $\sigma_\zeta(f)$, the kurtosis response spectrum$K_\zeta(f)$ was transformed to $\sigma_\zeta(f)$.

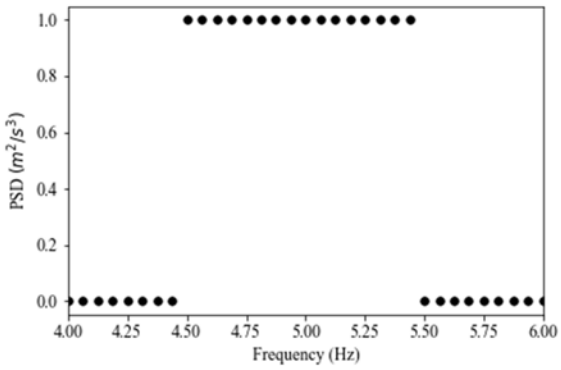

Fig. 3 Power Spectral Density to transform $K_\zeta(f)$ to $\sigma_\zeta(f)$.

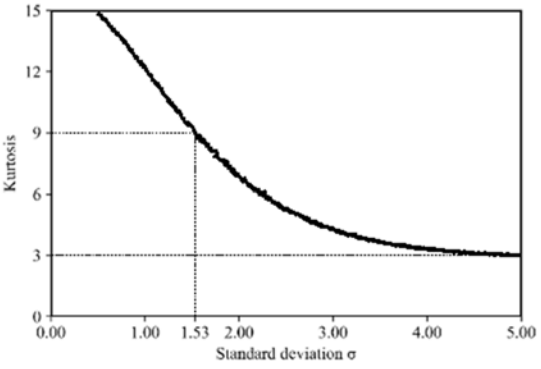

Fig. 4 The relationship between K_{a} and standard deviation σ to transform $K_\zeta(f)$ to $\sigma_\zeta(f)$.

The relationship between $\sigma_\zeta(f)$ and $K_\zeta(f)$ is needed to transform $K_\zeta(f)$ to $\sigma_\zeta(f)$. We generated a random vibration with PSD as shown in Fig. 3 using equation (9), (10), and (11). This PSD had energy from 4.5 to 5.5 Hz and $\Delta f = 1/16$ Hz. The standard deviation σ was from 0.05 to 5 and the acceleration kurtosis K_a was calculated for each value of σ (Fig. 4).

Then, the kurtosis response spectrum$K_\zeta(f)$ was calculated by equation (1) to (8). Fig. 5 shows the $K_{\zeta=0.07}(f)$ as an example of $K_\zeta(f)$. This $K_\zeta(f)$ was converted to $\sigma_\zeta(f)$ using Fig. 4. For example, $K_{\zeta=0.07}(f = 57\text{ Hz})$ is 9.0 in Fig. 5 and σ is 1.53 when the kurtosis is 9.0 in Fig. 4. Therefore, $\sigma_{\zeta=0.07}(56.5 \le f < 57.5)$ is set to 1.53.

Fig. 6 shows an example of the standard deviation $\sigma_{\zeta=0.07}(f)$. It is obvious that $\sigma_{\zeta=0.07}(f)$ is small at frequencies where $K_{\zeta=0.07}(f)$ is relatively large.

Fig. 7 shows an example of random numbers, of which the average is 8.0 and the standard deviation is $\sigma_{\zeta=0.07}(f)$. Δf was 1/16 Hz, and random numbers were generated 75 times for the same frequency.

Finally, random vibration was generated with the PSD of the real vibration and $\sigma_\zeta(f)$ by equation (9), (10), and (11).

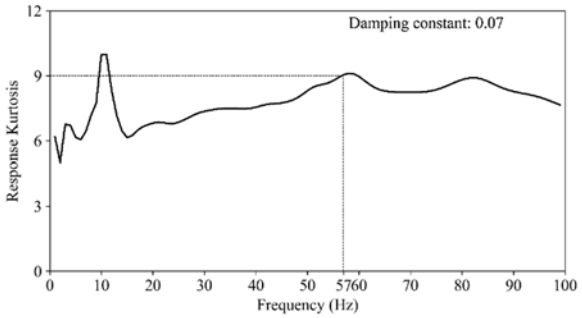

Fig. 5 Kurtosis response spectrum $K_{\zeta=0.07}(f)$.

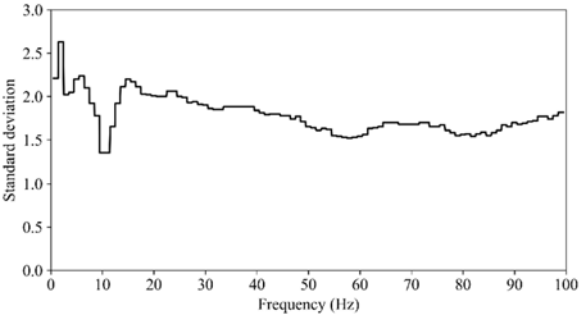

Fig. 6 Standard deviation $\sigma_{\zeta=0.07}(f)$.

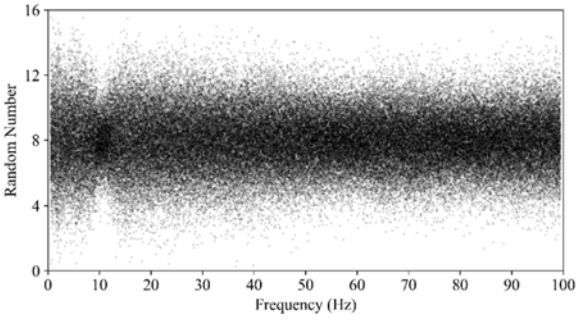

Fig. 7 Random numbers depending on $\sigma_{\zeta=0.07}(f)$.

4. Results and Discussion

4. 1 Effect of damping factor on the acceleration kurtosis and velocity kurtosis

Fig. 8 shows the relationship between the damping factor ζ and the kurtosis of the input acceleration $a(t)$ which is generated by proposed method. Both the acceleration kurtosis K_a and the velocity kurtosis K_v increase with increasing damping factor ζ. When ζ is 0.02, which is the minimum value as a factor of the proposed method in this study, both K_a and K_v are greater than 3. Therefore, all vibrations generated by the proposed method in this study are non-Gaussian. For the entire range of ζ in this study, K_a was slightly greater than K_v.

In this study, the vibration for which K_a had the same value as that of the real vibration (ζ=0.07), was chosen as a vibration for evaluation.

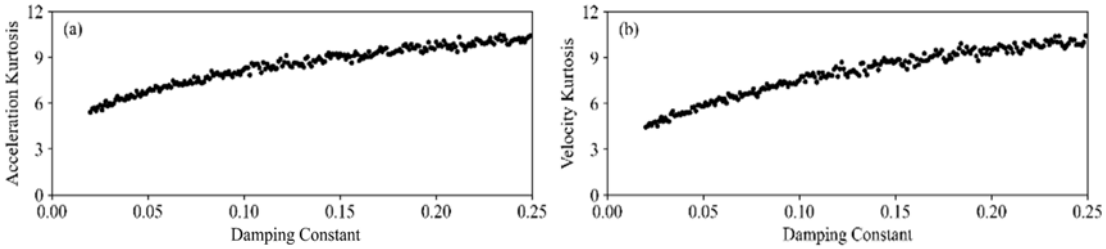

Fig. 8 Relationship between damping factor ζ and kurtosis, (a) acceleration kurtosis, (b) velocity kurtosis.

4. 2 Comparison of real and generated vibrations

In this study, the vibrations generated by the proposed method (T_d = 16 s, ζ = 0.07) and the previous method (T_d = 2 or 16 s) were compared with the real vibration.

Fig. 9 shows the time series acceleration of the real and generated vibrations. All of the vibrations were 1,200 s because the length of the real vibration was 1,200 s (Fig. 9 (a)). Comparing Fig. 9 (b) and (d), there are no significant differences between the proposed method and previous methods (T_d = 16 s). The envelope curve of Fig. 9 (c) is different from those of Fig. 9 (b) and (d) because of the difference in T_d.

Fig. 10 shows the time series velocity of the real vibration and generated vibrations. These velocities were integrated from the acceleration with low-cut filter (0.5 Hz) [11]. Almost all of the velocity peaks of the real vibration were less than 0.5 m/s, as shown in Fig. 10 (a). Comparing Fig. 10 (b) and (d), there are no significant differences between the proposed and previous methods (T_d = 16 s). The velocity peaks of the previous method (T_d=2 s) are smaller than those of the proposed method and the previous method (T_d= 16 s) as shown in Fig. 10 (b)-(d).

Fig. 11 shows the PSD of the acceleration. There were no significant differences between the real and generated vibrations.

Table 1 shows the statistical values of the real vibration and generated vibrations. There are no significant differences in the acceleration RMS and velocity RMS between the real vibration and generated vibrations. Also, there were no significant differences in K_a between the real and generated vibrations because they were generated as a target of K_a. The biggest difference between the vibrations was the K_v. The K_v value of the real vibration was 8.59 and greater than K_a. The K_v of the proposed method and the previous method (T_d= 16 s) were also slightly smaller than K_a. The K_v value of the proposed method (T_d= 2 s) was 3.65, which was much smaller than K_a.

Table 1 Statistical value of real vibration and generated vibrations.

	Acceleration RMS(m/s^2)	Velocity RMS(m/s)	Acceleration Kurtosis	Velocity Kurtosis
(a)Real Vibration	0.796	0.0804	7.24	8.59
(b)Proposed (T_d=16 s)	0.792	0.0800	7.20	6.59
(c)Previous (T_d= 2 s)	0.790	0.0832	7.24	3.65
(d)Previous (T_d= 16 s)	0.792	0.0798	7.18	6.41

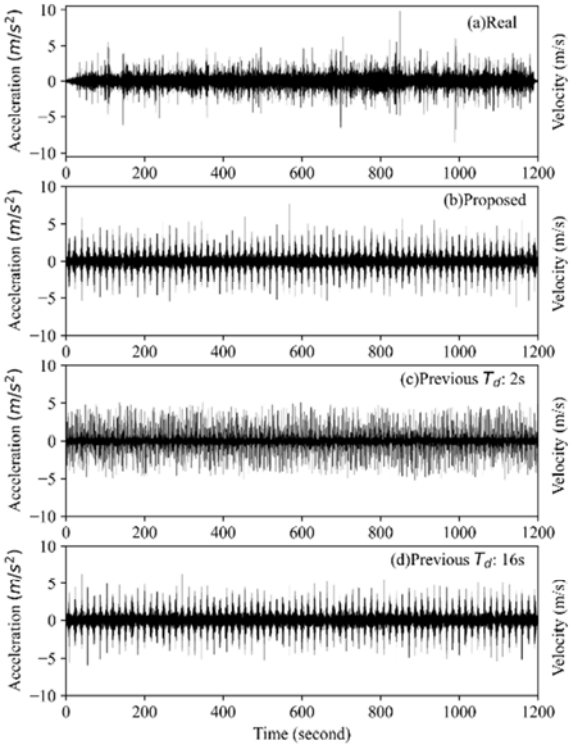

Fig. 9 Time series acceleration,
(a) real vibration, (b) proposed method,
(c) previous study method (T_d = 2 s),
(d) previous study method (T_d = 16 s).

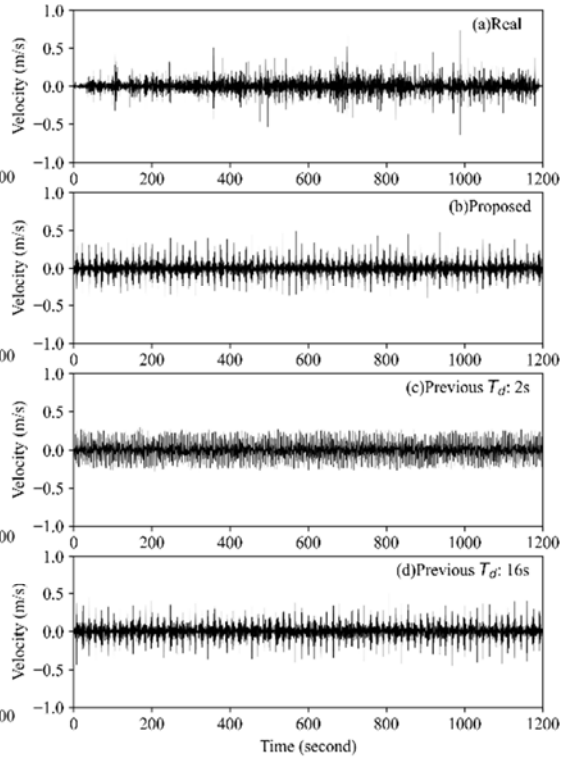

Fig. 10 Time series velocity,
(a) real vibration, (b) proposed method,
(c) previous study method (T_d = 2 s),
(d) previous study method (T_d = 16 s).

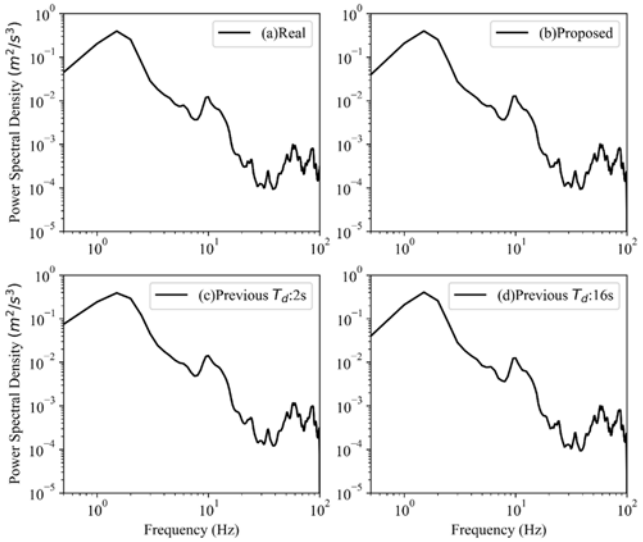

Fig. 11 Power spectral density of acceleration, (a) real Vibration, (b) proposed method,
(c) previous study method (T_d = 2 s), (d) previous study method (T_d = 16 s).

Fig. 12 shows the probability densities of the acceleration. The dotted lines show the Gaussian distributions. The mean parameter is zero, and the standard deviation are the values of acceleration RMS, as shown Table 1. All of the acceleration probability densities are non-Gaussian. In particular, the probability densities of the proposed and previous methods (T_d = 16 s) are quite similar.

Fig. 13 shows the probability density of the velocity. The dashed lines show the Gaussian distribution. The mean parameter is zero and the standard deviations are the values of the velocity RMS, as shown Table 1. The shape of the probability density of the previous method (T_d = 2 s) is quite different from the probability densities of the others. The probability densities of the real vibration, proposed, and previous method (T_d = 16 s) had the similar shapes. In particular, the probability densities of the proposed and previous methods (T_d = 16 s) were quite similar.

In terms of statistical values and probability densities, the only clear difference between real vibration and proposed method was K_v. Furthermore, there were almost no differences between the proposed and previous methods (T_d = 16 s) in terms of statistical values and probability densities.

Fig. 14 shows the RMS response spectra $R_\zeta(f)$. Since the lines almost overlapped in Fig. 14, it is considered that $R_\zeta(f)$ had almost the same results even if the vibration changed. When the damping factor ζ was small, $R_\zeta(f)$ changed significantly depending on the natural frequency, as shown in Fig. 14(a) and (b). As ζ increased, the difference in $R_\zeta(f)$ between the natural frequencies decreased.

Fig. 15 shows the kurtosis response spectra $K_\zeta(f)$. Higher values of $K_\zeta(f)$ resulted in the greater the damage to the product, even if $R_\zeta(f)$ remained the same. Therefore, the closer $K_\zeta(f)$ of a generated vibration is to that of the real vibration, the more it the vibration is assumed to be to the real vibration. The value of $K_\zeta(f)$ changed significantly depending on the natural frequency, especially in the case of a small damping factor ζ.

As shown Fig. 15(a), $K_{\zeta=0.04}(f)$ of the previous method (T_d = 2 s) was smaller than that of the real vibration in the low frequency region (<14 Hz). Conversely, $K_{\zeta=0.04}(f)$ of the previous method (T_d = 2 s) was greater than that of the real vibration in the high frequency region (>14 Hz). This result shows that the actual vibration could not be reproduced well just by making the value of K_a the same as that of the actual vibration.

The $K_{\zeta=0.04}(f)$ value of the previous method (T_d = 16 s), was close to a constant value regardless of the natural frequency except in the low frequency region. This tendency was not the same as the real vibration and the proposed method. The $K_\zeta(f)$ shape of proposed method was most similar to that of the real vibration among three generated vibrations, when damping factor ζ was 0.04 and the natural frequency $f_n$was around 10 Hz or above 50 Hz. For example, in the case of the real vibration, $K_{\zeta=0.04}(f = 10\ Hz)$ was 12.12, which was the maximum value in the range of natural frequencies from 1 to 100 Hz. In the case of the previous method (T_d = 2 or 16 s), $K_{\zeta=0.04}(f = 10\ Hz)$ were 5.23 and 6.84, respectively, which were much smaller than those of the real vibration. In the case of the proposed method, $K_{\zeta=0.04}(f = 10\ Hz)$ was 12.19, which was close to that of the real vibration.

When the damping constant was large (ζ = 0.12, 0.16), there was a small difference of $K_\zeta(f)$ between the real vibration and generated vibrations. Hence, the proposed method had the advantage in the case of a small damping constant (ζ = 0.04).

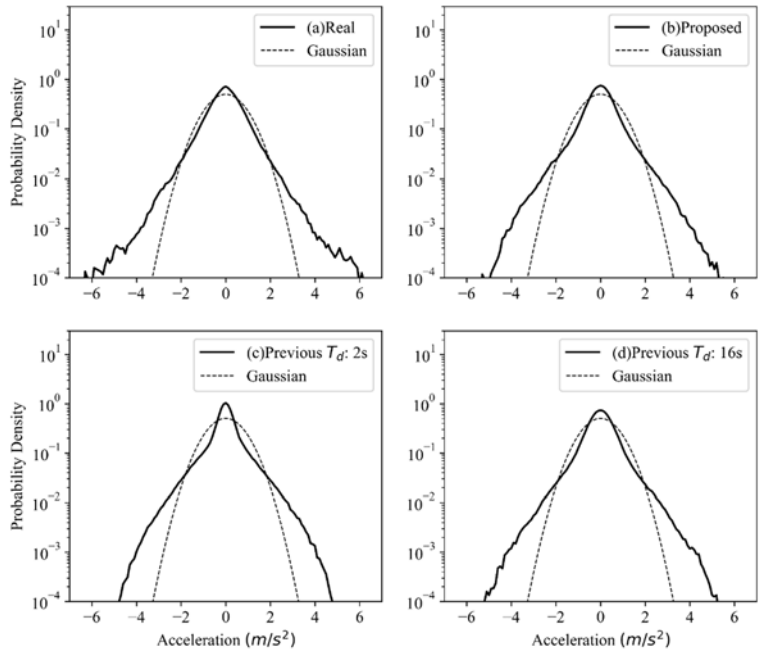

Fig. 12 Probability density of acceleration, (a) real vibration, (b) proposed method, (c) previous method ($T_d = 2$ s), (d) previous method ($T_d = 16$ s).

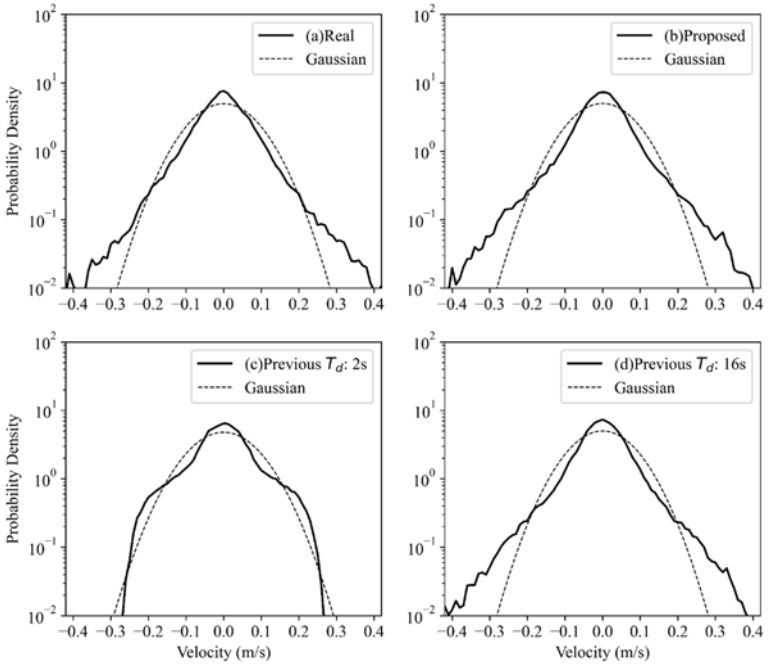

Fig. 13 Probability density of velocity, (a) real Vibration, (b) proposed method, (c) previous study method ($T_d = 2$ s), (d) previous method ($T_d = 16$ s).

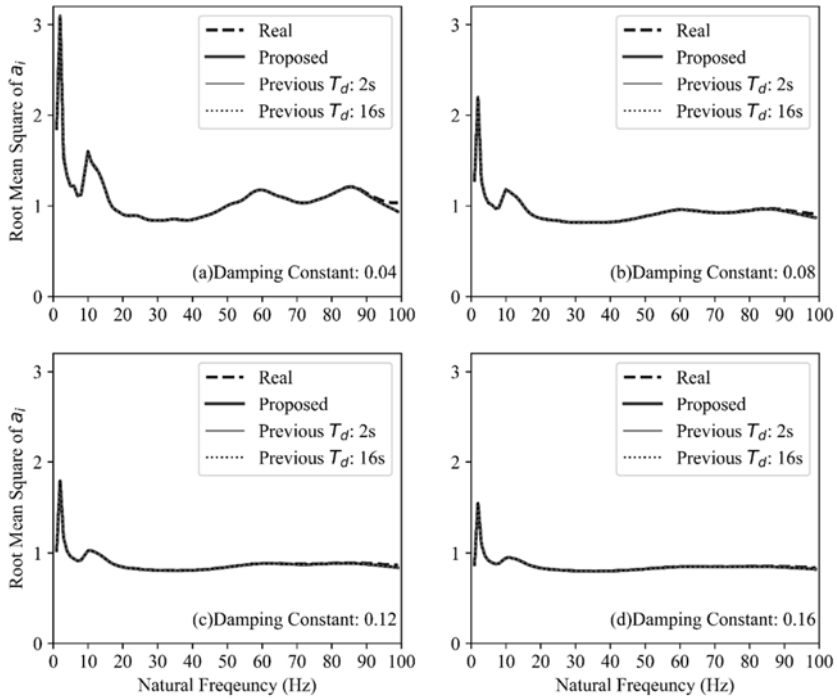

Fig. 14 Root Mean square response spectra of $a_i(t)$, (a) ζ=0.04, (b) ζ=0.08, (c) ζ=0.12, (d) ζ=0.16.

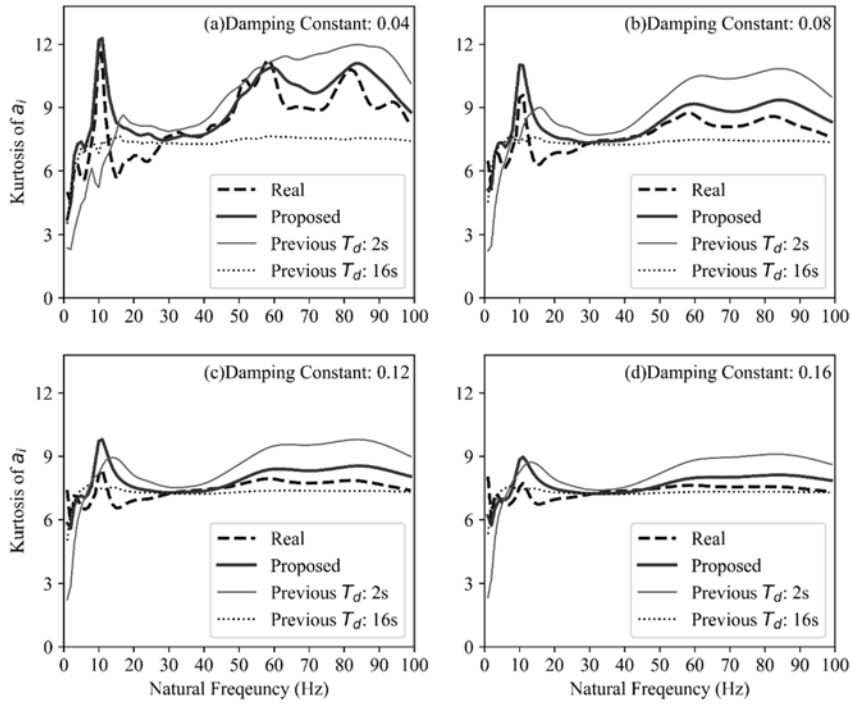

Fig. 15 Kurtosis Response spectra of $a_i(t)$, (a) ζ=0.04, (b) ζ=0.08, (c) ζ=0.12, (d) ζ=0.16.

5. Conclusions

Random vibration considering the kurtosis response spectrum was generated by the proposed method of changing the random number of the phase difference for each frequency. There were almost no differences between proposed and previous methods in terms of statistical values, probability densities, and RMS response spectrum. However, there were differences in the kurtosis response spectrum between the proposed and previous methods. From the point of view of the kurtosis response spectrum, the proposed method was an improvement compared with the existing one, especially when the damping constant ζ was 0.04. The proposed method needs to be closer to the real vibration when the damping constant is large (ζ = 0.12 and 0.16).

Acknowledgment

This work was supported by JSPS KAKENHI Grant Number JP18K04608.

References

1) J. Lepine, V. Rouillard and M.A. Sek, Review paper on road vehicle vibration simulation for packaging testing purposes, Packag. Technol. Sci., **28**(8), p. 672 (2015).
2) H. Zhou and Z-W. Wang, Measurement and analysis of vibration levels for express logistics transportation in South China, Packag. Technol. Sci., **31**(10), p665 (2018).
3) P. Böröcz1 and S. P. Singh, Measurement and analysis of delivery van vibration levels to simulate package testing for parcel delivery in Hungary, Packag. Technol. Sci., **31**(5), p342 (2018).
4) V. Rouillard, On the non-Gaussian nature of random vehicle vibrations, World Congress on Engineering, London, UK, p1219 (2007).
5) V. Rouillard and M. A. Sek, Synthesizing nonstationary, non-Gaussian random vibrations, Packag. Technol. Sci., **23**(8), p423 (2010).
6) S. R. Winterstein, Nonlinear vibration models for extremes and fatigue, Eng. Mech., **114**(10), p1772 (1988).
7) A. Hosoyama and T. Nakajima, The Method of Generating Non-gaussian Random Vibration Using Kurtosis, Packag. Sci. Technol., Jpn, **20**(1), p27 (2011).
8) D. Nakai and K. Saito, A method for generating random vibration using acceleration kurtosis and velocity kurtosis. J. Appl. Packag. Res., **11**(2), p64 (2019).
9) A. Hosoyama, K. Tsuda and S. Horiguchi, Development and validation of kurtosis response spectrum analysis for antivibration packaging design taking into consideration kurtosis. Packag. Technol. Sci., **33**(2), p51 (2020).
10) Harris' Shock and Vibration Handbook 6th.Edition, McGraw-Hill Education, p 8.2 (2009).
11) D. Nakai and K. Saito, Estimation method of velocity change on truck bed, J. Packag. Sci. Technol., Jpn, **28**(1), p. 33 (2019).

(Received 16Mach 2021)
(Accepted 8June 2021)

尖度応答スペクトルを考慮した ランダム振動の生成方法

中井 太地[*,**]、 斎藤　勝彦[*]

ランダム振動試験は、包装にとってトラック荷台での安全性を確認するため重要である。従来のランダム振動試験方法とトラック荷台の実際の振動には違いが存在する。この違いにより、過剰包装や過少包装が発生しうる。故に振動試験の入力振動を改善することは重要なテーマである。本研究では、尖度の応答スペクトルに焦点を当てた。先行研究で、実際の振動の応答尖度は固有振動数によって異なることが示されている。故に実振動と同じ尖度応答スペクトルを持つ試験振動は、実環境により近いと想定される。本研究では、尖度応答スペクトルを考慮して振動を生成させる方法を提案する。提案方法と今までの振動生成方法によって、PSD、RMS、加速度尖度、速度尖度は同じであるが、尖度応答スペクトルのみが異なる振動を生成した。実際の振動と生成された振動の間の尖度応答スペクトルを比較すると、提案手法は、特に減衰係数が小さい場合に改善効果が大きかった。

キーワード:　輸送、振動試験、尖度、応答スペクトル